

# Chapter 13

## A Human Augmentation Approach to Gait Restoration

Dino Accoto, Fabrizio Sergi, Nevio Luigi Tagliamonte, Giorgio Carpino, and Eugenio Guglielmelli

**Abstract** Impaired gait can be restored to its physiological level using wearable robotic systems acting alongside human lower limbs and providing assistive forces that adapt to the residual sensory-motor capabilities of the wearer. Such systems can be used as assistive aids (to overcome disabilities or age-related impairments) or as rehabilitation tools (to restore physical and neurological abilities through proper training). In order to elicit physiological gait as a behavior emerging from the interaction between the robot and the user, the robot morphology must be considered as an open design variable, thus relaxing the constraint of using basically anthropomorphic architectures. This chapter deals with several design aspects related to this approach for the development of lower limbs wearable robots. In particular, it analyzes kinematic compatibility issues, possible topological connections among robotic elements, morphological optimization of robot properties, actuation solutions with series compliance, interaction control schemes and user's intention detection strategies. Pilot tests on a novel non-anthropomorphic device, developed according to the proposed approach, are presented as a case-study, exemplifying the main design aspects described within the chapter.

**Keywords** Assistive and rehabilitation robotics • Wearable robotics • Exoskeleton • Compliant actuator • Physical human-robot interaction

---

D. Accoto (✉) • N.L. Tagliamonte • G. Carpino • E. Guglielmelli  
Università Campus Bio-Medico di Roma, via Alvaro del Portillo 21, 00128 Rome, Italy  
e-mail: [d.accoto@unicampus.it](mailto:d.accoto@unicampus.it); [n.tagliamonte@unicampus.it](mailto:n.tagliamonte@unicampus.it); [g.carpino@unicampus.it](mailto:g.carpino@unicampus.it);  
[e.guglielmelli@unicampus.it](mailto:e.guglielmelli@unicampus.it)

F. Sergi  
Rice University, Houston, TX 77005, USA  
e-mail: [fabs@rice.edu](mailto:fabs@rice.edu)

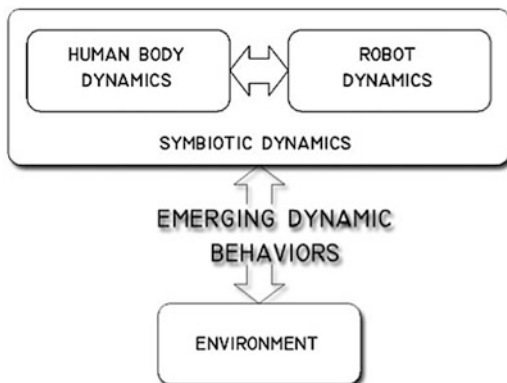
### 13.1 Human-Robot Symbiosis

Wearable robots (WRs) aim at supplementing the function of a limb (active orthoses and augmenting devices) or to replace it (prostheses). Wearability does not necessarily imply that the robot is ambulatory, portable or autonomous [1]. Historically, the earliest device resembling a WR was described by Yagn in the U.S. Patent granted in 1890 [2]. This wearable device, intended to augment human running and jumping capabilities, consisted of long bow/leaf springs operating in parallel to the legs, cyclically storing and releasing elastic energy according to gait phases. Several years later, General Electric Co. developed the concept of human-amplifiers (*Hardiman* project, 1966–1971).

Exoskeletons constitute a subset of WRs with specific characteristics. An exoskeleton is effectively defined in Dollar and Herr [3] as “*an active mechanical device that is essentially anthropomorphic in nature, is worn by an operator and fits closely to his or her body, and works in concert with the operator’s movements*”. In an anthropomorphic structure, robot kinematics is not a free design parameter. Conversely, WRs can be designed so to have a non-anthropomorphic kinematic structure. In fact, WRs are not just robots designed around the human body, so to obtain an as safe as possible physical Human-Robot Interaction (pHRI). Rather, the level of interaction between the WR and the human body should be advantageously pushed ahead by designing the WR so that a *symbiotic interaction* occurs between it and the human body. The adjective “symbiotic” refers to the intimate physical interaction between the human body and the robotic artifact, building upon the human capabilities in order to lead to useful *emergent behaviors*, assisting or augmenting the selected human performance (Fig. 13.1).

Specifically, *design for symbiosis* is intended as a kind of design for emergence aiming at producing dynamic behaviors, by augmenting wearer’s residual motor capabilities, as useful to a given purpose (e.g. restoring proper motor abilities in chronic subjects, of whom elderly people are the most socially relevant example).

**Fig. 13.1** Emerging behaviors, arising from the coupled dynamics of human body and robotic structure interacting with the environment, help the execution of a complex task with low computational efforts. Low-level adaptations to the environment are managed by the intrinsic properties of the mechanical structure of the robot (preflexes)



It is also desirable that the mechanical structure of the WR is capable of managing the low-level issues related to the interaction with the environment by exhibiting proper zero-delay, intrinsic responses (i.e. reflexes) to a perturbation [4]. The ability of a mechanical structure of producing useful emergent behaviors and of adapting itself to external perturbations through reflexes can be seen as whole as a form of *structural intelligence*, as an instantiation of *embodied intelligence*.

The concept of embodied intelligence highlights how intelligence benefits also from the physicality of an agent, where the term *physicality* is meant to catch as a whole the dynamic, kinematic and somesthetic properties of an organism and the typology of its possible interactions with the environment. Indeed, it is recognized [5] that the embodiment of an agent has implications on the information theoretic processes (e.g. by effectively structuring the sensory inflow from the environment) and that morphology itself can perform computation through physical interactions (i.e. morphological computation). Robots designed to exploit embodied intelligence are frequently simpler, more robust and adaptive than those based on the classical interaction control paradigm.

These concepts formulated in artificial intelligence and computer science are often strictly related with biological observations of animal behavior, especially in locomotion, that focus on the intimate connections among intelligence, morphology and performance. As shown in Kubow and Full [4], the lowest level of intelligence is completely physical, as it consists in the ability of neuro-musculoskeletal systems to present zero-delay, intrinsic responses to a perturbation [6]. Reflexes are useful for performing low-level tasks, such as stabilization and feedforward locomotion control. As an example, the cockroach *Blaberus discoidalis* is able to scramble over randomly distributed obstacles up to three times its body height without significantly slowing down [7]. Such striking performance cannot be achieved by a feedback-based, centralized sensory-motor control, because the required adaptation to the environment is too quick. On the contrary, robust locomotion is achieved mainly through a basically feedforward pattern applied to a properly tuned mechanical system. Such principles have been implemented in the development of a highly efficient hexapedal robot capable of sensorless robust locomotion at speeds up to 2.5 body lengths/s [8].

On a higher level, recent studies on biped robots have shown that even complex tasks, such as walking, may arise from the intrinsic dynamics of a machine during its interaction with the environment. Studies on passive walking show that bipedal walking, normally obtained through computationally demanding feedback control algorithms, can emerge from an accurate tuning of the dynamical properties of a purely mechanical system, without any feedback control [9, 10]. The performance obtained through this methodology produces a gait that appears to be more biomimetic under both the energetic and kinematic standpoints. In particular, it has been demonstrated that the energetic efficiency of such mechanisms is closer to that of the human body, while existing bipedal walking robots are about 30 times more energy demanding [11]. Moreover, experiments performed on physical simulation environments have shown that it is possible to optimize, via a coupled evolutionary

process, both the morphological properties of a robot and its controller, with mutual benefits for both, in terms of reduced complexity and enhanced efficiency [12].

The two examples mentioned above demonstrate that better performance, with lower computation cost and with simpler and lighter structures, can be achieved if the potentialities of structural intelligence are properly harvested and exploited. Till now, such concepts have been explored and applied to the development of robots inspired by a large variety of biological systems, such as mammals, fishes and insects. On the contrary, the human body has been poorly investigated from the structural intelligence standpoint, while this is a promising new route toward the development of useful machines intended for the strict interaction with humans, such as robots for rehabilitation, assistance and functional restoring for elderly and disabled people.

In the scenarios where the robot and the human body are strictly interacting, the design of the artificial system must take into account the dynamics of the biological counterpart, which is highly variable and actively tuned by the human sensory-motor system. When strict physical interaction occurs, the dynamics of the human body and that of the robotic artifact are strongly coupled. If the robot is meant to compensate for lost body functionalities, such as proper gait generation, the proposed approach consists in finding how the robotic system must be designed to take advantage of the variable biomechanical properties of the human body.

The objective is to design the robotic system in such a way that the dynamics of the human body, especially in the case of impaired or elderly subjects, and that of the robot during interaction, symbiotically benefit from each other, eliciting emergent dynamic behaviors, which favor the execution of the desired task.

The nature and the level of symbiosis, that can be effectively attained, depend on the specific employed design methods and tools and on their capability to accurately predict the kind of interaction that the user and the robot would establish, depending from the morphological and control properties of the latter.

The engineering of a specific dynamical interaction is still an open research objective. Indeed, it requires simulation tools not yet available, which should be capable to accurately model personal motor styles, human motor control strategies and time-dependent, subject-specific self-adaptations to the robot. Nonetheless, as presented in the following sections, the concept of structural intelligence can be effectively exploited to design a WR with a diverse structure, better ergonomics (i.e. intrinsically capable of solving micro- and macro- misalignments issues), better dynamical properties (e.g. limited inertial effects associated to the swinging of actuators), and good backdrivability.

The approach, in which embodied intelligence is taken a step further to embrace also the potentialities of structural intelligence, is radically new, as better highlighted by the analysis of the state of the art in the field of WRs, as summarized in the following section.

## 13.2 Wearable Robots for Gait Restoration

A substantial push in the advancements of the field of wearable robots for human performance augmentation has been provided by the program promoted by the US Defense Advanced Research Projects Agency (DARPA), called Exoskeletons for Human Performance Augmentation (EHPA), started in 2001, which encouraged the development of exoskeletons helping soldiers to carry backpacks during operative missions. The *Berkeley Lower Extremity Exoskeleton (BLEEX)* has been developed by prof. Kazerooni and his group at the University of California [13]. BLEEX features three Degrees Of Freedom (DOFs) at the hip, one at the knee, and three at the ankle. Of these, four are actuated: hip flexion/extension, hip abduction/adduction, knee flexion/extension, and ankle flexion/extension. Of the non-actuated joints, the ankle inversion/eversion and hip rotation joints are spring-loaded, and the ankle rotation joint is completely free [14].

After the first prototypal version of the system, the Berkeley Robotics & Human Engineering Laboratory worked on new versions of the device for military applications developing the *ExoHiker* and the *ExoClimber* systems, tailored for load carrying during overground walking or during slopes ascent. The third generation of their exoskeletal system, the *Human Universal Load Carrier (HULC)* has reduced bulkiness and weight, since structural parts are titanium made. Interestingly, the HULC is claimed to be the first system able to provide a reduction in the order of 5–15 % of the metabolic cost associated to overground walking.

*Sarcos* (recently purchased by Raytheon) has developed an exoskeleton also based on hydraulic actuation. The exoskeleton (*Sarcos XOS*) has been designed to encompass the entire body. The XOS robot includes 30 actuated DOFs and is controlled using a number of multi-axis force-moment transducers that are located between the feet, the hands and the torso of the operator and the machine [15]. However, the largest drawback of this device is the lack of a mobile power source. A quasi-passive exoskeleton, the *MIT exoskeleton*, has been designed in the Biomechanics Group at the Massachusetts Institute of Technology Media Laboratory by the group of prof. Hugh Herr. This concept seeks to exploit the passive dynamics of human walking in order to create a lighter exoskeletal device [11], which demonstrated an increased energetic efficiency when compared to conventional walking machine designed through a kinematically anthropomorphic design and controlled via Zero Moment Point (ZMP) technique [16, 17]. The group of prof. Yoshiyuki Sankai at the University of Tsukuba (Japan) developed an exoskeleton targeted for both performance-augmenting and rehabilitative purposes [18, 19]. The leg structure of the full-body *HAL-5* exoskeleton powers the flexion/extension of hip and knee joints via a DC motor with harmonic drive placed directly on the joints. The ankle dorsi/plantar flexion DOF is passive. The HAL-5 system utilizes a number of sensing modalities: skin-surface EMG electrodes, placed below the hip and above the knee on both the anterior (front) and posterior (back) sides of the wearer's body; potentiometers for joints angles measurement,

ground reaction force sensors, a gyroscope and accelerometer mounted on the backpack for torso posture estimation. HAL-5 is currently commercialized by the spinoff company Cyberdine (Tsukuba, Japan).

Compared to human augmentation devices, *mobile medical exoskeletons* are intended for assistive and/or rehabilitative purposes. Improving the quality of life of wheelchair users is the aim of the *Ekso*, designed and commercialized by the Ekso Bionics (Berkeley, CA, US), intended for people with lower extremity weakness or paralysis due to neurological disease or injury (spinal cord injuries, multiple sclerosis, Guillain Barré syndrome).

Founded in 2001 and originally operating under the auspices of the Technion Seed (Technion, Institute of Technology, Israel), Argo Medical Technologies has developed a robotic ambulation system for wheelchair users named *ReWalk*, assisting only the movements in the sagittal plane. The ankle joint is not actuated.

Different from Ekso and ReWalk, *REX*, produced by REX Bionics (Auckland, New Zealand), is an anthropomorphic lower body orthosis designed for sit-to-stand, stair ascend and overground walking, without the use of crutches. The system does not use sensors to sense the intention of the user but uses a joystick for the user to control the exoskeleton. The system has been validated with healthy subjects, and for sit-to-stand of wheelchair users.

The *Vanderbilt powered orthosis* [20] is a powered lower-limb orthosis intended for Spinal Cord Injured (SCI) individuals. Differently from the previous mentioned devices, it neither includes a portion worn over the shoulders, nor a portion under the shoes. The orthosis is intended to be used in conjunction with a standard ankle foot orthosis, which provides support at the ankle and prevents foot drop during swing.

*Treadmill-based WRs* are mainly used as rehabilitation platforms capable of (partially) supporting patient weight and of providing assistance in performing therapeutic exercises, usually according to the *Assist-As-Needed (AAN)* paradigm.

*Lokomat*, developed by Hocoma (Volketswil, Switzerland), assists hip and knee movements in the sagittal plane while the ankle joint is not supported. Similarly, the *LOPES (LOWER-extremity Powered ExoSkeleton)* is a treadmill-based wearable robotic device for gait training and assessment of motor function in stroke patients [21] developed at University of Twente by the group led by prof. Herman van der Kooij. It is comprised of two parts: the adjustable lightweight frame for pelvic control actuating the two horizontal pelvis translations and the exoskeleton leg with four actuated DOFs per each leg which assist hip flexion/extension, adduction/abduction, knee flexion/extension and ankle dorsi/plantar flexion. All the actuated DOFs are based on series elastic actuation, consisting of a servomotor, a flexible Bowden cable transmission and a force feedback controller. This solution implies that the actuators are used as force (and torque) sources and allow impedance control of the robot. Impedance control with this kind of setup can be used in both high impedance control (resembling position control) and zero impedance control.

The *AutoAmbulator* [22] by HealtSouth Corp. (AL, USA) essentially consists of an electrically actuated anthropomorphic device supporting hip and knee movements in the sagittal plane.

The *Pelvic Assist Manipulator (PAM)* and *Pneumatically Operated Gait Orthosis (POGO)* are pneumatic robots that compliantly assist in gait training. PAM can assist in five DOFs of pelvic motion, while POGO can assist the hip/knee flexion/extension [23]. The devices can be used in a back-drivable mode to record a desired stepping pattern that is manually specified by human trainers, then replay the pattern with compliant assistance. During compliant replay, the devices automatically synchronize the timing of the replayed motions to the inherent variations in the patient's step timing, thereby maintaining an appropriate phase relationship with the patient.

In some systems developed in the last years the principles of structural intelligence can be glimpsed. In Krut et al. [24], Mokhtarian et al. [25], Vallery et al. [26] passive spring-based balancers dynamically sustain the body weight during walking. In the *MIT SkyWalker* [27], passive walkers have provided inspiration to define gait rehabilitation strategies that promote natural legs dynamics during the swing phase. Another interesting example is the *Elastic exoskeleton* [28], developed at University of Michigan, where leaf springs provide intrinsic elasticity and allow an optimized human-robot energy exchange during running. In *KNEXO* [29] the principles of bioinspiration, as a form of embodied intelligence, has been exploited in the actuation system; the agonistic/antagonistic configuration of two pleated pneumatic artificial muscles has been adopted to actuate a knee orthosis for gait assistance.

The problem of assessing if, how and how much the findings achieved in the field of pseudo-passive bipedal walking can be transferred to the field of WRs for the lower limbs consists of a very tough challenge. Despite of that, the literature suggests that possible improvements of the performances of WRs can be provided by “opening” the design of the mechanical subcomponent, and not just focusing on novel control schemes or aspects related to actuators power efficiency or intrinsic safety.

These considerations suggest that WRs performances can benefit from a careful design of robot morphology, which is open in the case of non-anthropomorphic WRs, and can allow to achieve a better dynamical interaction with the human body and with the environment.

### 13.3 Non-anthropomorphic Design: From Topological Analysis to Morphological Optimization

The problem of optimal kinematic synthesis of non-anthropomorphic WRs may be very unpractical to be tackled by the conventional insight-driven engineering approach, due to the large number of open parameters involved in the design. This task can be simplified by automatic tools in support of the designer.

In the last decade, evolutionary programming has been applied to solve the problem of co-designing both the mechanics and the control of mobile artificial machines, by just defining the basic building blocks of the structure and the rules

to connect them [30, 31]. This open-ended design methodology has the advantage that it can lead to unexpected design solutions. However, such kind of methods implies that the entire design process is completely demanded to the tool, which can autonomously decide to switch to a more complex structure during the optimization phase so to increase the fitness of the best individuals.

The authors are pursuing a systematic approach for the kinematic synthesis of WRs, based on a three-step process. The first step requires the exhaustive search of all independent generalized solutions for a WR design problem; the subsequent step consists of the selection among the pool of admissible solutions; finally, a candidate solution is optimized in terms of its morphological parameters, to satisfy a multi-objective fitness function.

This three-step strategy appears more reliable compared to open-ended kinematic optimization approaches, since optimization algorithms, acting on a fixed parameter space, are simpler and converge faster. Compared to the “brute-force” approach followed in [30], this strategy guarantees that only a reduced subset of solutions are evaluated, i.e. those kinematically compatible with the human body. Additionally, this strategy assures *completeness*: all relevant generalized solutions (i.e. topologies) are considered before producing the final design. The only drawback of the approach consists in the fact it requires the a-priori knowledge of the independent topologies having desired kinematic properties. No standard design tool was available for this specific problem of the design of a non-anthropomorphic WR for gait assistance, and then a major methodological step has been focused on development of ad-hoc computational tools, adapted from the general case of mechanism design.

### ***13.3.1 Exhaustive Kinematic Synthesis of Non-anthropomorphic Wearable Robots***

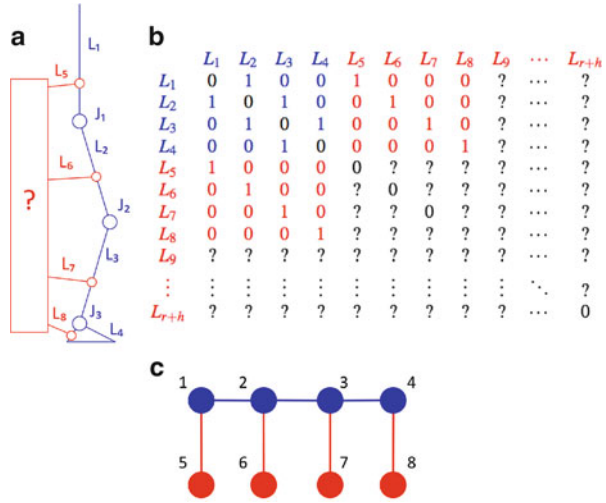
As a first step, it is important to define an efficient encoding, which allows the representation of the kinematic structure of a WR connected to a given human limb, which is modeled as a generalized serial chain. Since the aim is to evaluate also the mobility of the human limbs connected to the robot, the parallel kinematic chain, consisting of both robot links and human limbs, is considered. The most generalized level of abstraction at which such structure can be described is the *topology* level, which defines only the number of links and the connections among them.

#### **13.3.1.1 Kinematic Structure Encoding and Topologies Enumeration**

Under some reasonable hypotheses [32], many properties of mechanisms kinematics, such as the number of DOFs, are entirely determined only by the topology of the kinematic chain and unaltered by the geometry of its links. At this level of



**Fig. 13.2** Structural representation (a), generalized TAM (b) and graph representation (c) of the problem of structural synthesis of robotic orthoses for a planar WR for the lower limbs. Human articulations and segments are in blue, while robot links and joints are in red. In the adjacency matrix, the blue color is used to represent entries which describe the connectivity of human limbs, while the red color represents fixed entries



abstraction, the classical (graph)-(kinematic chain) analogy introduced in [33] can be employed, where graph vertexes correspond to the links of the chain and edges correspond to the joints. A graph can then be encoded through the Topology vertex-vertex Adjacency Matrix (TAM): a binary symmetric matrix of order  $n$  (where  $n$  corresponds to the number of links) where the element  $a_{ij}$  equals to 1 if link  $i$  and link  $j$  are connected through a joint, and to 0 otherwise.

As a first assumption, we decide to focus on planar kinematic chains composed of only revolute joints, for the assistance of the lower limb, modeled as a serial chain with three DOFs (hip, knee and ankle) moving in the sagittal plane. It is then unnecessary to discriminate on the type of joint connecting each link; hence the representation is complete in the description of kinematic chains topology, allowing the conversion of a problem of kinematic synthesis into a problem of graphs enumeration. The mentioned assumption limits the relevance of the methodology for the design of assistive WRs for the lower limbs, since the hip and the ankle joints have spatial movements. However, it can be noticed that, during ground walking, most of the power of the lower limbs is provided by actuation of movements in the sagittal plane, which is therefore the dominant plane during human locomotion [34].

The graph enumeration problem is graphically represented in Fig. 13.2, which depicts the structural representation, the graph representation and the corresponding TAM of the kinematic chain comprising both human segments and robot links. The process of enumerating kinematic chains consists of three successive steps: (i) enumeration of graphs with the desired mobility, (ii) pruning of isomorphic (i.e. non-independent) solutions and, (iii) pruning of non-kinematic compatible solutions. The mentioned steps will be described in more detail in the following.

Each kinematic solution can be represented by a graph with  $h + r$  edges, where  $h$  corresponds to the number of body segments (four in our case) and  $r$  corresponds to the number of robot links.

The complete list of independent kinematic solutions can be derived from the frame of the basic TAM shown in Fig. 13.2b. Any topology can be encoded by a binary string of length  $l$ , where:

$$l = h(r - h) + \frac{r(r - 1)}{2} \quad (13.1)$$

However, not any combination of parameters is adequate, since we are interested only in kinematic chains with a given number of DOFs. For a given planar kinematic chain with  $n$  links and  $f$  joints with one DOF, the total number of degrees of freedom (DOFs) is obtained by using the Kutzbach criterion [35]:

$$DOFs = 3(n - 1) - 2f \quad (13.2)$$

From (13.2), given any number of links and a desired number of DOFs, the kinematic chain can contain only a fixed number of joints. Since each joint between links  $i$  and  $j$  corresponds to a 1 in the  $(i, j)$  position of the corresponding TAM, the problem of enumeration of all topologies with a desired mobility can be converted into the problem of exhaustively listing the binary strings of length  $l$ , with a fixed number of ones.

### 13.3.1.2 Degeneracy and HR-Degeneracy Testing

A further selection over the list of enumerated topologies is performed, in order to filter out the kinematic chains which:

1. contain rigid or over-constrained sub-chains;
2. correspond to disconnected graphs (i.e. not all graphs vertices are connected by a path);
3. impair the motion of human joints.

A standard degeneracy testing algorithm has been implemented to recognize and discard rigid sub-chains (such as three links-three joints and five links-six joints sub-chains). Kinematic chains containing at least one sub-chain with zero or negative DOFs according to Kutzbach formula (e.g. three links-three joints and five links-six joints sub-chains) are considered as degenerate solutions and are then eliminated. Additionally, disconnected mechanisms (i.e. such that there is not a path connecting each couple of vertices of the corresponding graph) are eliminated with a purposely developed algorithm, which verifies the existence of a path between each couple of vertices.

Furthermore, an additional test was introduced so to exclude those solutions where a subset of  $p$  human joints is part of a subchain with less than  $p$  DOFs. In this

case the robot would impair human movements by imposing unnatural kinematic constraints. This test is called *HR-degeneracy test* (*Human-Robot degeneracy test*) since it applies to kinematic chains including both human and robot structures. The test is performed by recognizing the presence of sub-chains where two adjacent human joints are constrained in a one-DOF sub-chain, or where all three adjacent human joints are constrained in a two-DOFs sub-chain. The exhaustive list of such HR-degenerate primitives (reported in Fig. 13.2) could be obtained by adapting results coming from standard atlases of kinematic chains [36] and was re-obtained in a previous work concerning the enumeration of orthoses for a one-DOF human joint [37].

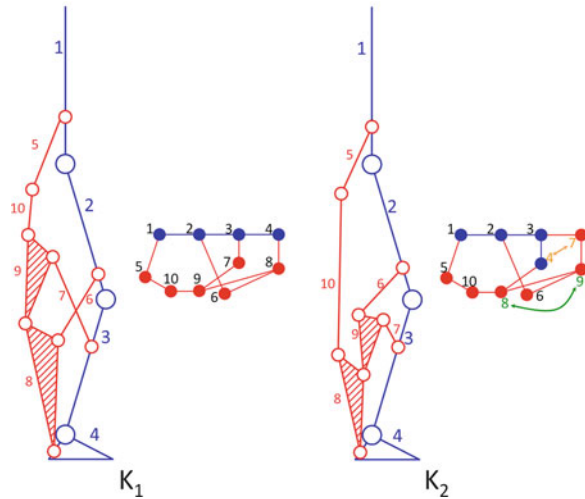
### 13.3.1.3 HR-Isomorphism Testing

Since the chosen method is based on the enumeration of suitable matrices of adjacencies, an explicit isomorphism test is required to guarantee mutual independence of set of enumerated solutions. Two kinematic chains  $K_1$  and  $K_2$  are said to be isomorphic if there exists a one-to-one correspondence between links of  $K_1$  and  $K_2$  such that any pair of links of  $K_1$  are jointed if and only if the corresponding pair of links of  $K_2$  are jointed. This means that from the graph corresponding to  $K_1$  one can obtain the graph corresponding to  $K_2$  by only relabeling link numbers.

A function defined on a kinematic chain is called an *index of isomorphism* if any given pair of kinematic chains is isomorphic if and only if the corresponding values of the function are identical. The *index of isomorphism* used in the present work is the characteristic polynomial of the Extended Adjacency Matrix (EAM)  $A^{(d)}$  of order  $d$ , as also suggested in [38]. In [38] it is demonstrated that the simultaneous evaluation of the characteristic polynomial of both  $A^{(0)}$ ,  $A^{(1)}$  and  $A^{(2)}$  has a reliability of 100 % for kinematic chains consisting of up to 11 links. This technique for isomorphism detection shows to be a very good compromise between reliability and computational efficiency, since it requires a polynomial time for assessing isomorphism.

However, when applying the isomorphism test to kinematic chains including both human segments and robot links, any kind of isomorphism test produces false-positives, because robot and human links would be treated the same way. This happens because isomorphism tests are “blind” with respect to the special condition which involves considering both human segments and robot links as part of a unique kinematic chain. A false positive happens any time the permutation, which maps one graph into the other, affects any of the human joints. From the perspective of designing a WR aimed at a certain kind of interaction with each of the human joints, such solutions correspond to actual different WR topologies and must not be discarded. An example of two isomorphic but not HR-isomorphic solutions is shown in Fig. 13.3. To recognize such kind of solutions, a modified version of the isomorphism test has been introduced and named *HR-isomorphism test* (since it applies to kinematic chain including both human and robot structures). This test basically consists of assessing, after a classical characteristic polynomial-based

**Fig. 13.3** Two isomorphic but not HR-isomorphic solutions. The permutation mapping  $K_1$  into  $K_2$  is given by the permutation vector [1 2 3 7 5 6 4 9 8]. This permutation maps link 4 (i.e. foot) into robot link 7. It can be noticed that local kinematic properties around each human joint (for example DOFs of the subchain including the hip, the knee and the ankle joints) are different in the two kinematic chains



isomorphism test, whether one of the permutations  $p_{adm}$  contained in a properly defined set  $P_{adm}$  is responsible for mapping one kinematic chain into another. Every permutation vector contained in the  $P_{adm}$  set is of the form  $p_{adm}(i) = [1 \ 2 \ 3 \ 4 \ perms_i(5:n)]$ , where the function  $perms_i$  provides the  $i^{th}$  element of the set of permutations of the elements in the input array.

### 13.3.2 Application to a Two-DOF Lower Limbs Wearable Robot for Hip and Knee Assistance

The developed method is applied to the design of the LENAR (Lower-Extremity Non-Anthropomorphic Robot) for hip and knee assistance in the sagittal plane. A design optimization is carried out to minimize static torques demanded to actuators to provide gait assistance. Due to the considerations reported above, the following hypotheses/constraints are imposed:

1. robot kinematic design is not fixed a-priori and can be possibly non-anthropomorphic;
2. only solutions involving revolute joints are considered;
3. the desired number of DOFs of the parallel structure, comprising both human segments and robot links, is two;
4. simultaneous and independent movements of the hip and the knee joints must not be constrained (i.e. the structure must not impose unnatural kinematic constraints to the addressed human joints).

The method described in Sect. 13.3.1 allowed to exhaustively list all the independent kinematic structures of planar kinematically-compatible wearable hip-knee robotic orthoses, respecting the constraints reported above. Ten generalized

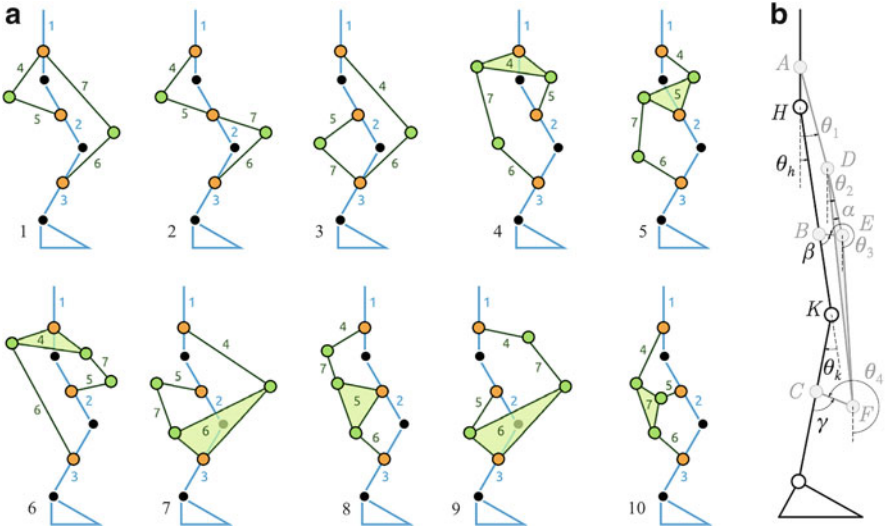


**Fig. 13.4** (a) Arbitrary structural representation of the ten generalized solutions for the design problem addressed. Human segments are reported in blue, and human articulations are reported in *black*. Robot joints are reported in *orange* (on attachment sites) and in *green* (Adapted from [39]). (b) Kinematic scheme of the selected WR design (*black*), worn by a subject (*gray*). Actuated joints are joints A and joint D, that guarantee controllability of hip posture and knee posture with two DOFs

solutions (topologies) are admissible in the considered design problem, as shown in Fig. 13.4. Such solutions represent the most synthetic form of describing the mechanical optimization problem described so far.

We applied a heuristic topology selection criterion based on a static ergonomics principle: correct force interaction in WRs is based on the transfer of forces to human segments only in the direction orthogonal to the bones. If the connection between a human segment and the robot is implemented through a binary passive link (i.e. with two passive revolute joints at its extremities), static forces applied on the human segments are necessarily directed along the connection link axis.

No forces along the orthogonal direction can be present, since no torque can be applied by passive joints. If said passive link is orthogonal to the human segment to which it is connected, the transfer of forces can be statically optimized based on simple geometric considerations (i.e. the attached link must be orthogonal to the addressed segment). Using this criterion, we investigated which of the ten topologies in Fig. 13.4 allowed links 5 and 6 (respectively connected to the thigh and shank) to be completely passive and orthogonal to human segments (labeled with 2 and 3). Three topologies (4, 6 and 10) guarantee in principle such condition, while still allowing independent control of hip and knee movements by actuating the two remaining joints. Topology 10 was finally selected, since it allows to reduce size and weight and to better distribute masses and inertias along the lower limb. A schematic of the resulting kinematic chain is shown in Fig. 13.4b.

### 13.3.2.1 Morphological Optimization of a Non-anthropomorphic Wearable Robot for Hip-Knee Assistance During Gait

A model of the chosen generalized solution was developed, as described in more detail in Sergi et al. [40], allowing to calculate the torques required to actuators to guarantee a physiological gait [34], for a generic set of parameters defining the structure shown in Fig. 13.4b. By using the mentioned model, morphological optimization was carried out, using a custom scalar fitness function, designed in order to take into account known limitations of actuators purposively developed for this wearable robot (Sect. 13.4), and in order to guarantee a high desired level of ergonomics of force interaction.

Using standard walking datasets reporting kinematic variables of level-ground walking (hip and knee angles  $\theta_h(t)$  and  $\theta_k(t)$ ), as well as inverse-dynamics calculated equivalent torques exerted by subjects (hip and knee torques  $\tau_h(t)$  and  $\tau_k(t)$ ), the corresponding actuator torques  $\tau_{m1}(t)$  and  $\tau_{m2}(t)$  and interaction forces at the points of contact  $A$ ,  $B$  and  $C$  could be calculated. In particular, the components of interaction forces in contact points  $B$  (shank) and  $C$  (thigh) were decoupled into the component perpendicular to the connected body segment  $F_{perp}$  and the component parallel to it  $F_{shear}$ .

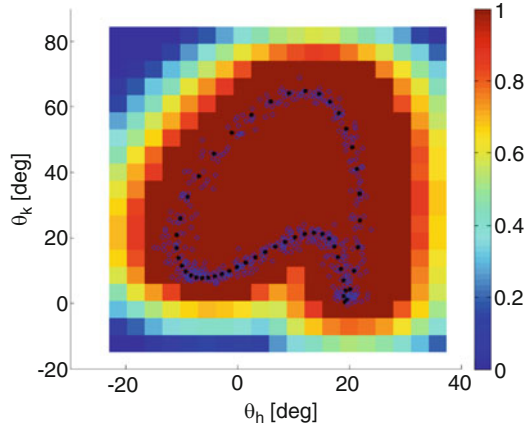
Workspace maximization was introduced as another optimization objective. In particular, increasing robustness of the design with respect to kinematic singularities was a highly sought design target, considered the specific application of the parallel WR. To this aim, passive angles values were individually checked for parallelism throughout the entire planar workspace of the robot. The occurrence condition of a singular configuration was that the angle between two passive links fell below a threshold, set to  $30^\circ$  in the optimization. Singularity is signaled by a binary variable  $sing(\theta_h, \theta_k)$ . The posture at which a singular configuration occurred was taken into account, by specifying a singularity weighting function  $w_{sing}(\theta_h, \theta_k)$ , designed to take into account the distance between the posture at which a singular configuration was detected and the nominal trajectory of the hip and knee joints during nominal gait, as shown in Fig. 13.5.

In order to account for both actuator limits on the maximum applicable torque, to avoid transfer of excessive interaction force along the supported segment axis and to increase robustness of the design with respect to singularities, the following scalar transfer functions were defined:

$$\begin{aligned}
 fitness_\tau &= \max(\tau_{m1}(t), \tau_{m2}(t)) / \tau_{max} \\
 fitness_F &= \max(F_{sh,B}(t), F_{sh,C}(t)) / F_{max} \\
 fitness_{sing} &= \sum_i \sum_j sing(\theta_{h,i}, \theta_{k,j}) \cdot w_{sing}(\theta_{h,i}, \theta_{k,j}), \quad (13.3)
 \end{aligned}$$

having defined the normalization values  $\tau_{max} = 50$  Nm and  $F_{max} = 30$  N. Solutions with singularities within the closed region defined by hip and knee profiles

**Fig. 13.5** Colormap of the weighting function  $w_{sing}$  used for weighting the occurrence of a singular posture during optimization. The weighting function is normalized in the range [0, 1] and assumes highest values inside the closed region defined by level-ground walking, in hip and knee angle coordinates, and degrades to smaller values, for postures more distant from an admissible posture during walking



during overground walking were discarded during optimization, and the remaining solutions were evaluated using the composite scalar fitness function, defined as:

$$fitness = fitness_t + fitness_F + fitness_{sing}. \quad (13.4)$$

A hybrid optimization strategy has been employed in order to explore the nine-dimensional space. The optimization algorithm consists of the consecutive application of a Genetic Algorithm (GA)<sup>1</sup> and a deterministic constrained non-linear optimization (CNLO)<sup>2</sup> method (using MATLAB `fmincon` function). The latter was used to perform a local optimization, using the best individual produced by the Genetic Algorithm as starting point. The fittest solution was selected for the final design, and the resulting relevant functions considered in the optimization are described in Fig. 13.6. The optimized solution requires a peak actuator torque of 52 Nm for level-ground walking of a subject with mass 80 kg, compared to peak hip and knee torques, calculated via inverse kinematics, equal to 48 Nm. Furthermore, the maximum shear force transferred to the supported body segments equals 21 N. The optimized solution was fabricated and integrated with custom designed actuators, as detailed in the next sections.

<sup>1</sup>GA parameters: Population Size: 40, Max Generations: 100, Scattered Crossover with Fraction: 0.8, Elite count: 2, Migration Fraction: 0.4, Migration Interval: 5, Stall Generations Limit: 15, Function Tolerance:  $10^{-5}$ .

<sup>2</sup>The “active-set” algorithm was used. Maximum number of iterations: 100, Parameters Termination Tolerance:  $10^{-9}$ .

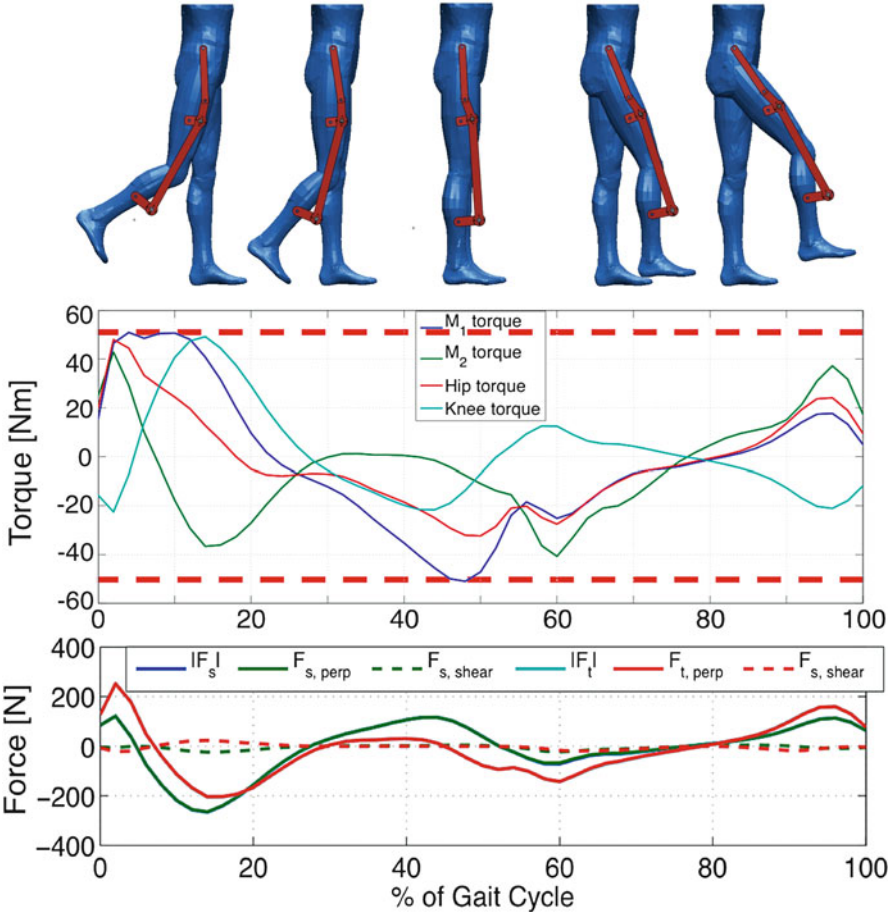


**Fig. 13.6** (Top) Poses of the mechanism during different phases of a walking cycle. Profiles of (middle) actuator torques and (bottom) forces at the attachment points *B* (shank) and *C* (thigh), for the optimized solution corresponding to the inverse dynamics simulation of the system, for level-ground walking of a subject with mass equal to 80 kg

### 13.4 Compliant Actuators and Joints

The need of a safe pHRI is crucial in assistive WRs, which are not required to simply move the limbs according to prescribed patterns, but should offer an amount of assistance adapted to the residual motor capabilities of the subjects. In this case a high level of biomechanical compatibility and dynamical adaptability is desirable. These machines have to be as transparent as possible to the active motion of the users and to provide assistance as needed in conditions where they are not able to complete a prescribed motor task. The need to stably and robustly regulate human-robot dynamic interaction, also on the basis of the variable level of assistance



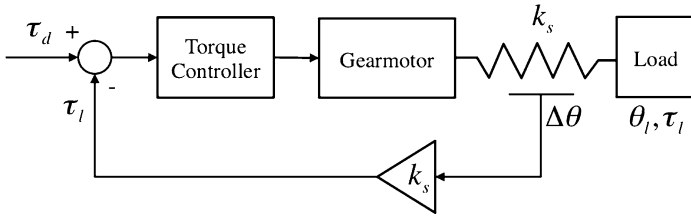


**Fig. 13.7** Torque control scheme for a rotary SEA.  $\tau_d$  represents the desired torque,  $k_s$  the stiffness of the series elastic element,  $\Delta\theta$  the spring deflection,  $\tau_l$  the output torque and  $\theta_l$  the output angle

required by the subjects, entails the use of actuators operating in an ideal force (or torque) mode control. This implies theoretical zero output impedance (i.e. perfect back-drivability) and high force (torque) control fidelity.

The smart inclusion of springs in the mechanical structure can effectively reduce both the power and energy requirements demanded to an actuator [41, 42]. This is because a spring can store and release energy efficiently during cyclic repetitive tasks. Reproducing passive elastic properties of human and animal joints can also enormously improve the energetic efficiency of legged robot, especially in the case of running and hopping machines, as demonstrated in pioneer works in the early 1980s both in simulation and in prototypal implementations [43].

The interposition of a compliant element between an actuator and its load was originally presented in Pratt and Williamson [44] and Pratt et al. [45]. The proposed prototype, named Series Elastic Actuator (SEA), was a linear actuator. A number of rotary systems have been developed in recent years [40, 46–53] (Fig. 13.8).

SEAs provide several advantages:

- shock tolerance;
- motor inertia is decoupled from the output link;
- the compliant element protects the motor and gearbox in case of impacts;
- output torque/force can be calculated from the measure of the elastic element deflection;
- the effects of stiction, friction, backlash and other non-linearities are reduced;
- work and power output of the actuator can be increased if an appropriate series elasticity is selected according to a specific task;
- in cyclical and/or explosive tasks efficient energy storage/release can be achieved;
- the high-frequency impedance of the actuator is limited to the stiffness of the elastic element.

Rotary SEAs are typically torque-controlled, using the representative control scheme depicted in Fig. 13.7. In this general scheme, the spring deflection  $\Delta\theta$  provides an estimate of the torque exerted by the actuator  $\tau_l$ ; this measure is used as feedback signal for torque control.

The stiffness of the series elastic element must be carefully selected in order to trade-off between performances, adaptability and safety. Moreover, the dimensions

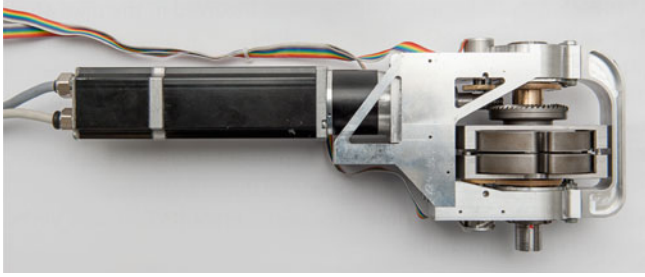


**Fig. 13.8** Rotary SEA developed for the LENAR Peak torque: 55 Nm; torque control bandwidth: 5.0 Hz. The custom-designed spring pack has a rotary stiffness of 272.3 Nm/rad. The interaction force is measured with a quantization of  $2.6 \times 10^{-2}$  Nm, using two 15 bit absolute encoders

and weight of the spring have to be reduced as much as possible, especially for wearable robotics applications. In order to be included in a torque control scheme, a compliant element for a SEA is then required to be verified against the maximum output torque supplied by the actuator and to possibly provide a linear torque vs. rotation relationship both in static and dynamic conditions to guarantee an accurate torque estimation and consequent control performance. Several solutions in literature have been proposed to overcome these design challenges. To implement the desired output torsional stiffness some authors have adopted linear compression springs to mimic a torsional stiffness [50, 54–56], while others have used compliant elements embedded in the transmission train or custom torsional springs directly connected to the load [46, 47, 49, 57].

Nevertheless, series elasticity causes a degradation of performances in terms of control bandwidth with respect to traditional rigid actuation systems [58]. This limitation can be overcome using elastic elements whose properties can be varied during operation. The aim of independently regulating motion and impedance field to improve performances as well as stably controlling robots interaction forces with external agents have steered to the development of *Variable Stiffness/Impedance Actuators (VSA/VIA)*, which are obtained by means of redundant actuation solutions [59, 60], i.e. including a number of active elements higher than the number of actively controlled DOFs.

Finally, impedance may be tuned by resorting to passive joints, with tunable mechanical impedance [61, 62].

## 13.5 Control

The control of WRs must assure that users' limbs are not forced towards harmful configurations and that no dangerous forces are imparted. Additionally, user's motion intentions have to be accommodated, shaping the action of the robot around subject's residual sensory-motor capabilities, behavior and motor style.

To this aim traditional stiff position-controlled robots and pre-defined motion patterns become inadequate and interaction control schemes, underlying proper force modulation, intention recognition and adaptation features have to be adopted. This is even more critical if a restoration of physiological behaviors based on subject-specific features is targeted.

### 13.5.1 *Interaction Control*

Conventional approaches to achieve direct or indirect force modulation [63] include: (i) *Explicit (or direct) force control* [64]: a force servo is implemented since the desired force is directly regulated closing a force feedback loop. (ii) *Stiffness and damping control* [65]: where a virtual spring or damper is created around an equilibrium position. (iii) *Impedance control* [66], generalizes the concepts of stiffness and damping controls. The position and velocity are commanded to follow an equilibrium trajectory and the controller modulates robot behavior as a viscoelastic or as a second-order system (if also virtual inertial contribution is considered). Control gains, setting virtual stiffness, damping and inertia, directly correlate with stability and bandwidth. (iv) *Hybrid position/force control* [67] combines position control, employed in unconstrained directions, with force control in interaction with external agents (e.g. obstacles). More sophisticated control algorithms can be basically considered as an evolution of these basic schemes.

In kinesthetic robotics [68] an alternative to impedance control is constituted by admittance control, which consists in measuring interaction forces to display desired admittance through position servos. This strategy allows displaying high virtual stiffness and mass but it asks for high positioning bandwidth, and hence for high-power and high-impedance actuators. Impedance controlled robots typically lack performance in kinesthetic display of high impedance but this is not critical in robotic physical assistance since no extremely stiff contact or large mass/inertia have to be displayed. For these reasons impedance control is commonly preferred.

Impedance control allows variable deviation from reference trajectory depending on the user's performances and provides comfortable assistance since robots are not perceived as too rigid or obtrusive. Therefore, high-impedance mode is used when the subjects need a high level of assistance and, in the worst case, they are completely unable to move (a predefined kinematic pattern has to be rigidly imparted). On the other hand, in low-impedance mode the subjects must be guided and assisted with a weak intervention and without altering their natural motion. Ideally they should not be hindered when null impedance is set and the robot is desired to be fully transparent. In the control of WRs these two opposite behaviors have to be guaranteed, both for therapeutic reasons in rehabilitation scenarios and for adaptation to different levels of disability in assistance applications.

The stability of interaction control schemes depends on the dynamic characteristics of the robot and of the interacting system. Pioneering studies on direct force control of manipulators explored sources and solutions to instabilities caused

by interactions with the environment (*coupled instability*) [69, 70]. In Colgate and Hogan [69] it was shown that a robot, which is stable when no interaction occurs (*isolated stability*), can exhibit unstable behaviors when interacting with passive environments, such as springs or masses. A simplified analysis on linear, time-invariant systems in Colgate and Hogan [69] showed that a (force) feedback controlled plant is stable during interaction if it has the interaction port behavior of a passive system, i.e. the transfer function of the impedance at the interaction port is a positive real function. This condition basically quantifies the concept that the system, for any time period, cannot deliver more energy at its interaction port than that introduced into it. This condition is valid for interactions with arbitrary stable, passive environments. Passivity-based control laws guarantee robust performance with respect to uncertainties and they can be used for a safe pHRI [71]. Even though passivity criterion ensures stability only with passive environments, the successful interaction with the human motor system (basically non-passive because of time delays in sensory feedback loops) is due to the limited frequency content and energy production of active human motion [72]. Hence, since the magnitude of human limbs impedance is quite bounded, passivity criterion, as stability measure, may be often regarded as overly conservative.

### 13.5.2 Control of Compliant Actuators

Impedance control demands actuators to be ideal force/torque sources. To this aim, it is useful to decouple the dynamics of the actuator and the load by intentionally interposing a compliant element. The introduced series elasticity complicates both the actuator design and control, reducing the controllable bandwidth due to saturation effects that limit the maximum achievable motor velocity in deflecting the spring [58].

Different approaches to SEA control have been proposed in literature. First solutions were based on the regulation of motor current with feed-forward compensation of motor inertia [73]. Current regulation was replaced by position control in Pratt et al. [74] while in Wyeth [55] a velocity loop nested in an external torque loop was proposed, thus considering the motor as an ideal velocity source. In Kong et al. [75] torque regulation was based on a PD controller coupled to a disturbance observer that compensated for model errors and plant variations. A similar model-based approach was presented in Grun et al. [76].

Passivity conditions for the control of SEAs based on inner velocity control loop was derived in Vallery et al. [77]. It was demonstrated that for stiffness-controlled SEA, the maximum renderable stiffness equals the physical stiffness of the series elastic element, if conservative demands for passivity are to be met.

### ***13.5.3 Robot Adaptation and Intention Detection***

WRs have to adapt to cognitive and motor capabilities of the users. In the case of assistance for motor (e.g. gait) restoration, residual functions have to be taken into account, similarly to what happens in neuro-rehabilitation, where the active participation of the subject is crucial to optimize motor recovery (AAN paradigm, [78, 79]). On the other side, a non negligible factor is also the adaptation of the user to the external robotic agent: the human learning capability causes a re-modulation of muscular activity to cope with and benefit from the external assistive actions exerted by the robot [80] reducing the effort in performing a task but simultaneously keeping the control of the device. Therefore, human-robot coupled adaptation is fundamental mechanism to be taken into account.

From these considerations it is clear that strategies to detect user's intention and to synchronously adapt robot behavior in a natural and smooth fashion are strongly needed. A possible intention detection strategy consists in using interfaces with the central or peripheral nervous system ([81]; Velliste et al.). Nevertheless, these solutions are highly invasive and implants are not yet sufficiently reliable/durable.

A number of controllers based on the measurements of electromyographic signals (EMG) have been explored [82–84]. These controllers estimate the muscular force, and consequently the joint torque, from EMG measurements, using model-based [85] or model-free [86] approaches, and provide assistive torques as a fraction of the one to be exerted by the subject. EMG-based approaches can pose some issues in terms of signal acquisition, subject-specific calibrations (intra and extra experimental sessions), electrode positioning, and skin condition. Moreover, model-based torque estimation is computationally demanding, sensitive to subject anatomy and to electrodes placement. Anyhow, compared to inverse dynamics techniques, EMG-based methods do not require dynamic models of the limbs and of their interaction with the environment/robot.

Another interesting approach to predict the limbs motion consists in extracting kinematic anticipatory information from the movements of different body district using wearable sensors. In particular, biomechanical and motor control studies evidenced that the movements of the human body segments are dynamically coupled [87] (e.g. postural stability during walking can only be achieved by the upper and lower body coordination). For example, the upper body (especially head and arms) motion has a natural anticipatory informative content with respect to locomotion activities, which can be exploited to improve the detection of human intention and to regulate the controllers of WRs, thus achieving simpler and more natural adaptation to the human. In the field of gait analysis, wearable sensors have quickly advanced and networks able to perform even complex tasks, such as fall detection, have been developed [88]. In the same way it is possible to estimate voluntary intention to start and stop walking. When gait is initiated, the user objective changes from staying in a stationary position to achieving the balance needed to stabilize walking. Gait termination is characterized, on the other hand, by increased braking forces of the lead foot and by a reduction of trail foot push-off during the final steps. Based on

these kinds of information, in Novak et al. [89] a method to detect gait initiation and termination using inertial measurement units, sensorized insoles and machine learning algorithms was presented.

Another promising and non-invasive approach, useful in case of periodic motion, consists in predicting movements directly from the observation of joint kinematics [90]. The strategy exploits the concept of motor primitives, i.e. the idea that complex motor behaviors can be described as the composition of simple elementary blocks. A non-linear dynamical system can be derived able to synchronize itself with complex human movements with a finite set of parameters. This system is based on Adaptive Frequency Oscillators (AFOs), mathematical tools developed in Righetti et al. [91] for many applications [92]. An AFO is expressed as a dynamical system characterized by a limit cycle. Its parameters (amplitude, frequency, phase, etc.) can adapt to an external input, such as the human kinematics, thus reflecting the real-time user intention about the performed movement. This approach has been successfully used to control upper and lower body exoskeletons [93].

### 13.6 Experimental Tests with a Compliant Non-anthropomorphic WR

In this section we report on tests exemplifying the main aspects presented in the previous sections. In the tests, performed on healthy subjects, a stiffness-controlled non-anthropomorphic robot with SEAs establishes a symbiotic interaction with the user, by predicting walking kinematics through the observation of residual voluntary movements (further details can be found in Tagliamonte et al. [94]).

The LENAR, depicted in Fig. 13.9, is composed (for each leg) of: (i) Supporting links, whose kinematic structure been designed starting from the optimization process described in Sect. 13.3. (ii) Two rotary SEAs connected to joints  $A$  and  $D$ ; (iii) Cuffs at the pelvis level (joint  $A$ ), at the thigh level (joint  $B$ ) and at the leg level (joint  $C$ ). The segment  $EF$  can be manually adjusted to make robot kinematics to be compatible with different users. Other regulations (position of the joints  $A$ ,  $B$  and  $C$  on the pelvis cuff, the thigh cuff and the leg cuff respectively) are allowed by sliders.

The treadmill-based platform is shown in Fig. 13.10. The WR is suspended to a support system able to passively compensate its weight, without introducing resonance frequencies so to minimize the inertia perceived by the subjects. Cables are used to connect the weight balancing system to the pelvis cuff. Hip and torso rotations are unconstrained.

Each of the four SEAs is torque-controlled. The employed control scheme is based on the cascaded approach proposed in Vallery et al. [95], and described in Sect. 13.5. The robot is stiffness-controlled in the joints space. The torque for each actuated joint (right  $r$  and left  $l$  leg) is set as:

$$\tau_{mi,d}(t) = -k_{mi} [\theta_{mi}(t) - \theta_{mi,d}(t)] \quad (13.5)$$

**Fig. 13.9** Blank circles,  $H$  and  $K$ , represent the human hip and knee joints respectively.  $A$  and  $D$  are the actuated robotic joints, also indicated as  $m_1$  and  $m_2$

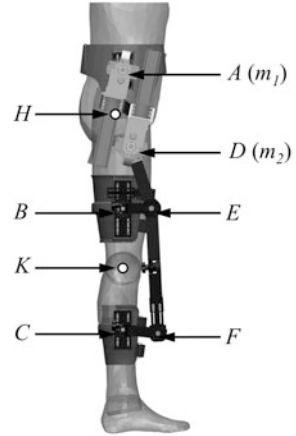
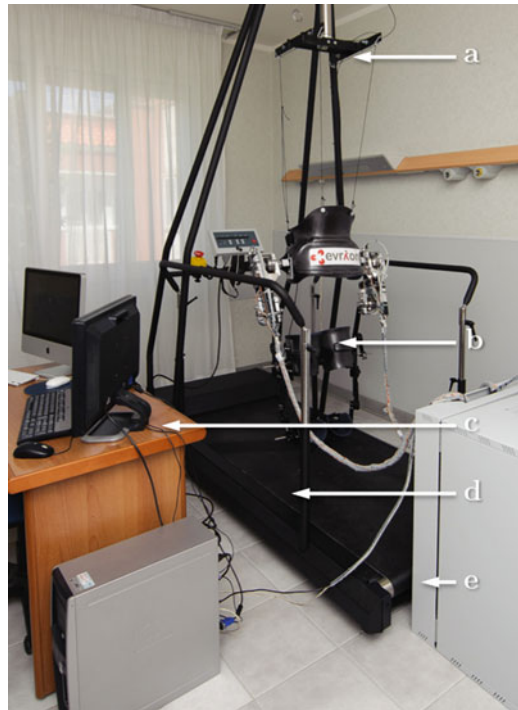


**Fig. 13.10** Treadmill-based platform. (a) Robot weight support system; (b) Wearable robot; (c) Control station; (d) Treadmill; (e) Electronic rack



with  $\theta_{mi}$  and  $\theta_{mi,d}$  actual and desired actuators rotations respectively,  $k_{mi}$  the virtual stiffness ( $i = 1, 2$ ).

The block scheme of the control of a single SEA is represented in Fig. 13.11.

Assistive torques are provided following the approach proposed in Ronsse et al. [93], based on a pool of AFOs, which learn periodic joints angles  $\theta(t)$  in steady-

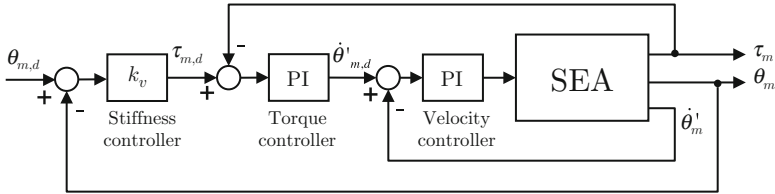


**Fig. 13.11** SEA control scheme.  $\tau_m, \theta_m$  are the output torque and angle respectively;  $\dot{\theta}'_m$  is the motor velocity. Torque controller generates a desired velocity value  $\dot{\theta}'_{m,d}$  as set-point for the velocity controller. Stiffness controller generates a desired elastic torque with virtual stiffness  $k_v$ .

state conditions. In addition, the oscillators are coupled to a non-linear filter, a sum of weighted Gaussian-like kernels as a function of the phase. An iterative local regression continuously learns the weights to estimate joint angle  $\hat{\theta}^*(t)$ . Therefore, joint angle at a time corresponding to  $\Delta\phi$  phase lead in the future  $\hat{\theta}^{*,\Delta\phi}(t)$  is derived. For each joint the assistive torque is calculated as in (13.5) by setting  $\theta_{mi,d} = \hat{\theta}_{mi}^{*,\Delta\phi}$ . With this approach the user is attracted by elastic torques towards her/his estimated future kinematic status, having the possibility to continuously adapt the frequency and the amplitude/shape of the attractive pattern.

Experimental tests were performed to assess torque tracking capabilities of the SEAs. The output shaft of each actuator was connected to a torque sensor to measure torques delivered, while measuring spring deflections. Torques and deflections data were fitted, obtaining a stiffness of  $270.2 \pm 3.1$  Nm/rad. Torque control regulation was evaluated by connecting the output shaft of the SEA to the frame (i.e. considering the deflection of the elastic element without any external load disturbances). The transfer function between desired and actual torque was determined by using a non-parametric identification method [96] and setting as desired torque a waveform with a flat spectrum in the range 0.1–10 Hz and peak torque 15 Nm. An almost flat transfer function was found, with an amplitude attenuation of 3 dB at about 6.5 Hz.

To estimate the order of magnitude of the torques needed to actuate the robot in the free space, physiological walking movements were produced with the robot not worn. Results demonstrated that necessary torques were lower than 12 % of the maximum allowable of the actuators (mainly gravitational and friction effects had to be compensated since the test was performed at slow walking speed) while the remaining 88 % is available to provide physical assistance.

A voluntary healthy subject (male, 28 years old, height 180 cm, body mass 80 kg), was asked to walk on the treadmill wearing the robot suspended to the weight support system. Cuffs were fastened to minimize their relative motion during trials but also to assure user's comfort. Before the tests, the subject was asked to freely walk at a self-selected walking speed for 10 min (robot unpowered) to get familiar with the device.

Back-drivability tests aimed at evaluating robot intrinsic transparency, i.e. at verifying that a human subject can walk physiologically even though the robot is



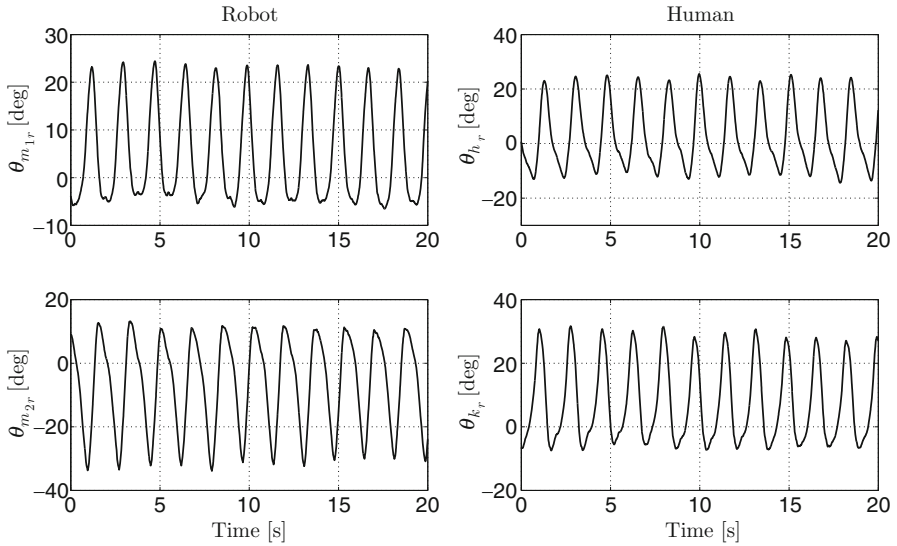


**Fig. 13.12** Robot actuator and human joint rotations for the back-drivability test performed at a walking speed of 2.5 km/h. Representative data for the right leg, in steady-state conditions, are reported

unpowered. For this test, actuators were turned off and the user had to back-drive the robot at different walking speeds (2.0, 2.5 and 3.0 km/h). Robot actuated joints rotations ( $\theta_{mir}$  and  $\theta_{mil}$ ,  $i = 1, 2$ ) and human-robot interaction torques in the robot joint space ( $\tau_{mir}$  and  $\tau_{mil}$ ,  $i = 1, 2$ ) were recorded; angles ( $\theta_h$  and  $\theta_k$ ) and torques ( $\tau_h$  and  $\tau_k$ ) in human joint space were calculated. In Fig. 13.12 robot actuators and human joints angles of the right leg are reported for a representative test at a walking speed of 2.5 km/h. The Gait Cycle (GC) for this test (calculated averaging on ten periods) is 1.71 s. Interaction torques for the same test, average and standard deviation calculated on ten cycles, are reported in Fig. 13.13 in human joint domain.

Back-driving torques were found to be in the order of 10 Nm (i.e. 15–20 % of torques delivered by human joints during overground walking). This result demonstrates the low mechanical impedance of the actuated joints (SEAs).

In assistance tests the subject was initially asked to walk freely at a self-selected walking speed (2.5 km/h), with robot actuators switched off. In this phase, AFOs could learn kinematics in the robot joint space  $\hat{\theta}_{mi}^*$  and calculate it with a predefined phase lead in the future (set to 10 % of the gait cycle). A representative kinematic prediction is reported in Fig. 13.14.

Estimated kinematics only requires few gait cycles to converge to the actual profiles. In Fig. 13.15 torques delivered by the four actuators during assistance test are depicted. At  $t = 24.5$  s assistance is enabled and virtual stiffness is set as  $k_{mil} = k_{mir} = k_v$  ( $i = 1, 2$ ). Then, its value is manually changed as reported in the lower graph of the Fig. 13.15. Modifying virtual elasticity corresponds to changing

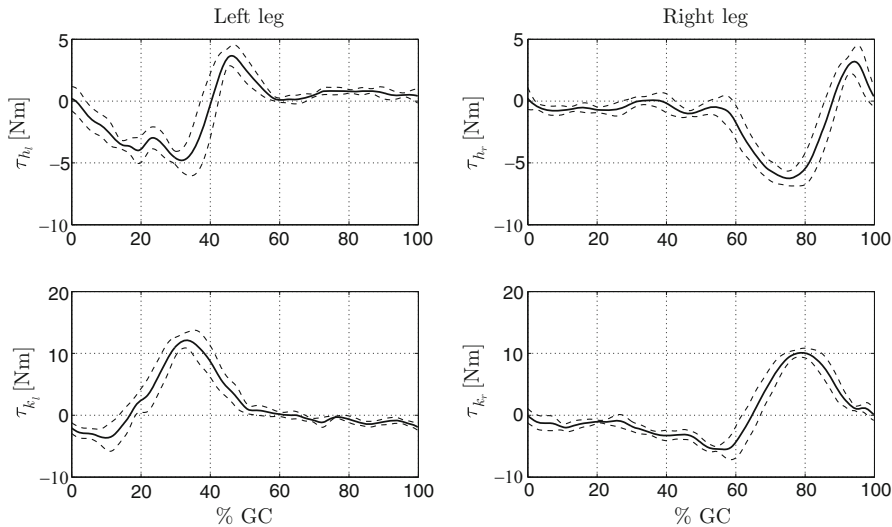


**Fig. 13.13** Human-robot interaction torques in the human joint space (as a function of the percentage of the GC) for the back-drivability test performed at a walking speed of 2.5 km/h. Data are averaged over ten gait cycles. Solid line: mean torque; dashed lines: standard deviation

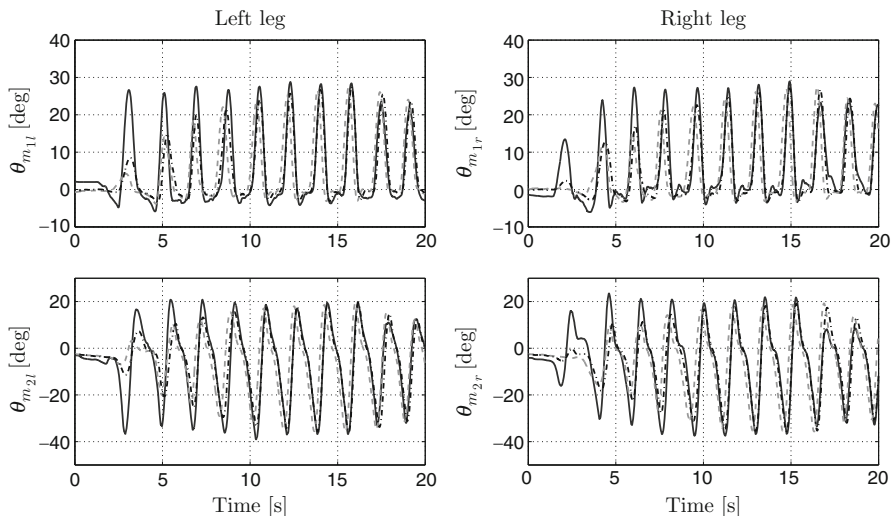


**Fig. 13.14** AFO-based kinematic estimation in the robot joint space with actuators switched off during a test at 2.5 km/h walking speed. Solid line: measured angle; dashed black line: estimated angle; dashed gray line: predicted (shifted) angle. The phase shift is set to 10 % of the GC

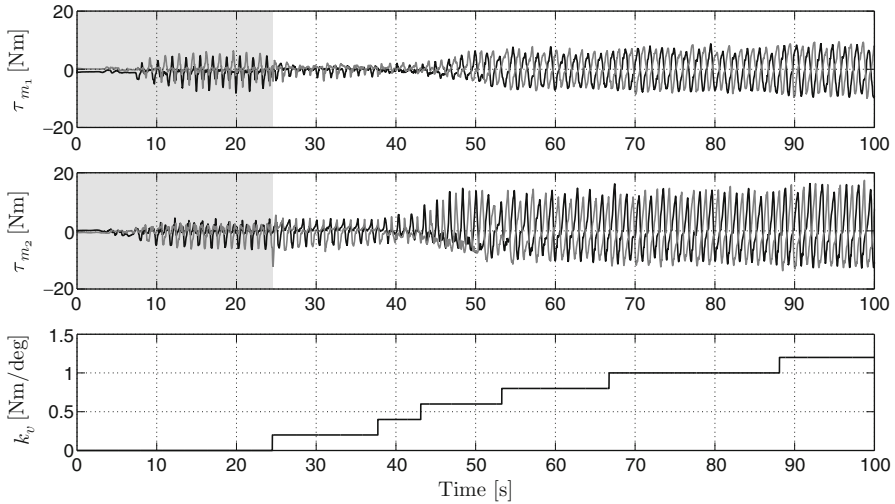


**Fig. 13.15** Actuator torques delivered during the assistance test. *Black line*: right leg; *Gray line*: left leg; *Gray band*: unassisted mode (actuators powered off). At  $t = 24.5$  s assistance is enabled. Virtual stiffness was manually changed as reported in the lower graph

assistance level, since the robot produces physical support with a more or less rigid behavior. Starting from the case of disabled actuators, interaction torques initially reduced for low values of assistance, then increased, producing assistance.

## 13.7 Conclusions

Design is a creative activity, inherently centered on the designer's technical insights. Whereas conventional design methodologies are effective in several application fields for robotics technology, a number of issues arise in the case of WRs, since they have to cope with the human body own dynamics, influenced by a number of concurrent biomechanical, physiological and neurological factors, sometimes not yet completely understood.

An emerging design paradigm for robotic systems is based on Embodied Intelligence, i.e. on the idea of introducing some level of morphological computation in the structural subsystem of a mechatronic machine. This approach tends to allocate some basic control function to the "body" of the robot, for simplifying the higher levels of control and reducing the need for embedded sensors and computational units.

The concept of Embodied Intelligence also applies to the human body, which can be considered as one of the most advanced examples of 'biomechatronic' system capable of performing useful morphological computation to improve its own performance while interacting with the environment. This appears particularly

evident in the case of walking, where the biomechanics of the lower limbs and the synchronized movements of the arms assure smooth periodic energy exchanges between the muscular springs, the body mass and the environment, leading to limit cycles which correspond to proper walking patterns. This concept has been, and is being, intensively investigated for the development of walking bipedal robots, where the design of a mechanical structure, endowed with the proper dynamics, greatly simplifies the achievement of desired behaviors.

In the case of WRs, the human body and the robot have to be treated as a symbiotic system, where the biological and the artificial components dynamically interact with each other (e.g. exchanging assistive forces) and, as a single whole, with the external environment. In this scenario, the artificial component has to be designed so that the symbiotic compound system (human + robot) exhibits the desired emerging behaviors, such as a physiologically restored gait. Since this behavior is elicited, and not imposed by the machine, this approach intrinsically builds upon the residual motor capabilities of the user. In this sense, gait restoration in elderly and/or disabled people is obtained by augmenting the (possibly limited) residual capabilities of the user. This approach, inherently open-ended since the topology/morphology of the robot has to be considered as a design variable, is computation intensive, and relies on modeling and optimization tools. As such, also the model of the biological component (i.e. the user) is central. The development of such a model still appears as a major research challenge, deserving intense efforts.

Indeed, the open-ended design approach needs to take into account biomechanical constraints, such as kinematic compatibility, and technological limitations in the fabrication of the actual device. In this chapter these aspects were addressed presenting methods to enumerate possible human-compatible topological solutions and to optimize morphological parameters. Technological actuation solutions exploiting intrinsic compliance were presented. Interaction control schemes and intention detection strategies were also discussed.

As a case-study of the presented design aspects, some pilot tests on a newly developed non-anthropomorphic robot were reported, demonstrating some of the potentialities of the novel design methodology proposed by the Authors. In this regards, re-engineering the traditional machine design cycle in order to exploit the potentialities of Embodied Intelligence can be considered as a major, novel and promising research avenue, whose exploration is only at its beginning.

## References

1. Pons JL (2008) *Wearable robots: biomechatronic exoskeletons*. Wiley, Chichester
2. Yagn N (1890) Apparatus for facilitating walking, running and jumping. US Patent 420179
3. Dollar AM, Herr H (2007) Active orthoses for the lower-limbs: challenges and state of the art. *Transp* 1:968–977
4. Kubow T, Full RJ (1999) The role of the mechanical system in control: a hypothesis of self-stabilization in hexapedal runners. *Phil Trans R Soc Part B* 354:849–861

5. Pfeifer R, Lungarella M, Iida F (2007) Self-organization, embodiment, and biologically inspired robotics. *Science* 318:1088–1093. doi:[10.1126/science.1145803](https://doi.org/10.1126/science.1145803)
6. Brown IE, Loeb GE (2000) *Biomechanics and neuro-control of posture and movement*. Springer, New York
7. Full RJ, Tu MS (1990) Mechanics of six-legged runners. *J Exper Biol* 148:129–146
8. Cham JG, Bailey SA, Cutkosky MR (2000) Robust dynamic locomotion through feedforward-preflex interaction. In: *ASME International Mechanical Engineering Congress & Exposition (IMECE 2000)*, Orlando, Florida, November 5–10, pp 5–10
9. Collins S, Wisse M, Ruina A (2001) A three-dimensional passive-dynamic walking robots with two legs and knees. *Int J Robot Res* 20:607–615
10. McGeer T (1990) Passive dynamic walking. *Int J Robot Res* 9(2):62–81
11. Collins S, Ruina A, Tedrake R, Wisse M (2005) Efficient bipedal robots based on passive-dynamic walkers. *Science* 307:1082–1085. doi:[10.1126/science.1107799](https://doi.org/10.1126/science.1107799)
12. Matsushita K, Yokoi H, Arai T (2006) Pseudo-passive dynamic walkers designed by coupled evolution of the controller and morphology. *Robot Autonomous Syst* 54:674–685. doi:[10.1016/j.robot.2006.02.016](https://doi.org/10.1016/j.robot.2006.02.016)
13. Kazerooni H, Steger R, Huang L (2006) Hybrid control of the Berkeley lower extremity exoskeleton (BLEEX). *Int J Robot Res*. doi:[10.1177/0278364906065505](https://doi.org/10.1177/0278364906065505)
14. Zoss A, Kazerooni H, Chu A (2006) Biomechanical design of the Berkeley lower extremity exoskeleton (BLEEX). *IEEE/ASME Trans Mechatronics* 11:128–138
15. Jacobsen SC (2007) On the development of XOS, a powerful exoskeletal robot. In: *IEEE/RSJ International Conference on Intelligent Robots and Systems*, October 29–November 2, San Diego, USA
16. Vukobratovic M, Borovac B (2004) Zero-moment point – thirty five years of its life. *Int J Human Robots* 1:157–173
17. Vukobratovic M, Juricic D (1969) Contribution to the synthesis of biped gait. *IEEE Trans Biomed Eng* 16:1–6. doi:[10.1109/TBME.1969.4502596](https://doi.org/10.1109/TBME.1969.4502596)
18. Kawamoto H, Lee S, Kanbe S, Sankai Y (2003) Power assist method for HAL-3 using EMG-based feedback controller. In: *IEEE International Conference on Systems, Man and Cybernetics*, Waikoloa, Hawaii, USA, October 10–12, 2005. ISBN 0-7803-9298-1, vol 2, pp 1648–1653
19. Suzuki K, Kawamura Y, Hayashi T et al (2006) Intention-based walking support for paraplegia patient. In: *2005 IEEE International Conference on Systems, Man and Cybernetics*, Waikoloa, Hawaii, USA, October 10–12, 2005. ISBN 0-7803-9298-1, vol 3, pp 2707–2713
20. Farris R, Quintero H, Goldfarb M (2011) Preliminary evaluation of a powered lower limb orthosis to aid walking in paraplegic individuals. In: *IEEE transactions on neural systems and rehabilitation engineering*, p 1, doi: [10.1109/TNSRE.2011.2163083](https://doi.org/10.1109/TNSRE.2011.2163083)
21. Veneman J, Kruidhof R, Hekman E et al (2007) Design and evaluation of the LOPES exoskeleton robot for interactive gait rehabilitation. *IEEE Trans Neural Syst Rehabil Eng* 15:379–386. doi:[10.1109/TNSRE.2007.903919](https://doi.org/10.1109/TNSRE.2007.903919)
22. Fisher S, Lucas L, Thrasher TA (2011) Robot-assisted gait training for patients with hemiparesis due to stroke. *Top Stroke Rehabil* 18:269–276. doi:[10.1310/tsr1803-269](https://doi.org/10.1310/tsr1803-269)
23. Aoyagi D, Ichinose WE, Harkema SJ et al (2007) A robot and control algorithm that can synchronously assist in naturalistic motion during body-weight-supported gait training following neurologic injury. *IEEE Trans Neural Syst Rehabil Eng* 15:387–400. doi:[10.1109/TNSRE.2007.903922](https://doi.org/10.1109/TNSRE.2007.903922)
24. Krut S, Benoit M, Dombre E, Pierrot F (2010) MoonWalker, a lower limb exoskeleton able to sustain bodyweight using a passive force balancer. In: *2010 IEEE international conference on robotics and automation (ICRA)*, Anchorage, Alaska, May 3–8, pp 2215–2220
25. Mokhtarian A, Fattah A, Agrawal SK (2010) A novel passive pelvic device for assistance during locomotion. In: *2010 IEEE international conference on robotics and automation (ICRA)*, Anchorage, Alaska, May 3–8, pp 2241–2246

26. Vallery H, Duschau-Wicke A, Riener R (2010) Hiding robot inertia using resonance. In: 2010 annual international conference of the IEEE engineering in medicine and biology society (EMBC), August 31–September 4, 2010, Buenos Aires, Argentina, pp 1271–1274
27. Bosecker CJ, Krebs HI (2009) MIT-Skywalker. In: 2009 IEEE international conference on rehabilitation robotics, ICORR 2009, 23–26 June 2009, Kyoto, Japan, pp 542–549
28. Cherry MS, Kota S, Ferris DP (2009) An elastic exoskeleton for assisting human running. In: Proceedings of the ASME 2009 international design engineering technical conferences & computers and information in engineering conference, IDETC/CIE 2009, August 30, San Diego, USA, pp 1–12
29. Beyl P, Knaepen K, Duerinck S et al (2011) Safe and compliant guidance by a powered knee exoskeleton for robot-assisted rehabilitation of gait. *Adv Robot* 25:513–535
30. Lipson H, Pollack JB (2000) Automatic design and manufacture of robotic lifeforms. *Nature* 406:974–978
31. Sims K (1994) Evolving virtual creatures. In: Proceedings of the 21st annual conference on computer graphics and interactive techniques, New York, pp 15–22
32. Dobrjanskyj L, Freudenstein F (1967) Some applications of graph theory to structural analysis of mechanisms. *J Eng Ind-Trans ASME Ser B* 89:153–158
33. Mruthunjaya TS (2003) Kinematic structure of mechanisms revisited. *Mech Mach Theory* 38(4):279–320
34. Winter DA (1999) Biomechanics and motor control of human gait: normal, elderly and pathological, 2nd edn. University of Waterloo Press, Waterloo
35. Kutzbach K (1929) Mechanische Leitungsverzweigung. *Maschinenbau, der Betrieb*
36. Ding H, Huang Z (2007) A unique representation of the kinematic chain and the atlas database. *Mech Mach Theory* 42(6):637–651
37. Sergi F et al (2010) A systematic graph-based method for the kinematic synthesis of non-anthropomorphic wearable robots. In: 2010 IEEE conference on Robotics Automation and Mechatronics (RAM), pp 100–105
38. Sunkari RP (2006) Structural synthesis and analysis of planar and spatial mechanisms satisfying Gruebler's degrees of freedom equation. Department of Mechanical Engineering, University of Maryland, College Park
39. van den Kieboom J, Sergi F, Accoto D, Guglielmelli E, Ronsse R, Ijspeert AJ (2011) Co-evolution of morphology and control of a wearable robot for human locomotion assistance exploiting variable impedance actuators. *Procedia Comput Sci* 7:223–225
40. Sergi F, Accoto D, Carpino G et al (2012) Design and characterization of a compact rotary series elastic actuator for knee assistance during overground walking. In: 2012 4th IEEE RAS EMBS international conference on biomedical robotics and biomechatronics (BioRob), 24–27 June, Rome, Italy, pp 1931–1936
41. Hurst J, Rizzi A (2004) Physically variable compliance in running. CLAWAR, Springer-Verlag, [www.springeronline.com](http://www.springeronline.com)
42. Raibert MH, Tello ER (1986) Legged robots that balance. *IEEE Expert* 1:89. doi:10.1109/MEX.1986.4307016
43. Raibert MH (1984) Hopping in legged systems – modeling and simulation for the 2D one-legged case. *IEEE Trans Syst Man Cybernetics* 14:451–463
44. Pratt G, Williamson M (1995) Series elastic actuators. *Proc IEEE/RSJ IROS* 1:399–406
45. Pratt GA, Willisson P, Bolton C, Hofman A (2004) Late motor processing in low-impedance robots: impedance control of series elastic actuators. In: American control conference, Boston, pp 3245–3251, 30 June–2 July 2004
46. Kong K, Bae J, Tomizuka M (2011) A compact rotary series elastic actuator for human assistive systems. In: IEEE/ASME transactions on mechatronics, pp 1–10, ISSN: 1083-4435, doi: 10.1109/TMECH.2010.2100046
47. Lagoda C, Schouten A, Stienen A et al (2010) Design of an electric series elastic actuated joint for robotic gait rehabilitation training. In: 2010 3rd IEEE RAS and EMBS international conference on biomedical robotics and biomechatronics (BioRob), 26–29 September, Tokyo, Japan, pp 21–26, doi: 10.1109/BIOROB.2010.5626010

48. Sensinger J, Weir R (2008) User-modulated impedance control of a prosthetic elbow in unconstrained, perturbed motion. *IEEE Trans Biomed Eng* 55:1043–1055. doi:[10.1109/TBME.2007.905385](https://doi.org/10.1109/TBME.2007.905385)
49. Stienen A, Hekman A, Ter Braak H et al (2010) Design of a rotational hydroelastic actuator for a powered exoskeleton for upper limb rehabilitation. *IEEE Trans Biomed Eng* 57:728–735. doi:[10.1109/TBME.2009.2018628](https://doi.org/10.1109/TBME.2009.2018628)
50. Tsagarakis N, Laffranchi M, Vanderborght B, Caldwell D (2009) A compact soft actuator unit for small scale human friendly robots. In: 2009 IEEE international conference on robotics and automation, ICRA'09, 12–17 May, Kobe, Japan, pp 4356–4362, doi:[10.1109/ROBOT.2009.5152496](https://doi.org/10.1109/ROBOT.2009.5152496)
51. Veneman J, Ekkelenkamp R, Kruidhof R et al (2005) Design of a series elastic- and Bowden cable-based actuation system for use as torque-actuator in exoskeleton-type training. In: 2005 9th international conference on rehabilitation robotics, ICORR 2005, June 28–July 1, Chicago, Illinois, pp 496–499, doi: [10.1109/ICORR.2005.1501150](https://doi.org/10.1109/ICORR.2005.1501150)
52. Wyeth G (2006) Control issues for velocity sourced series elastic actuators. In: Proceedings of Australasian conference on robotics and automation 2006, December 6–8, Auckland, New Zealand
53. Accoto D, Carpino G, Sergi F, Tagliamonte NL, Guglielmelli E (2013) Design and characterization of a novel high-power series elastic actuator for a lower limb robotic orthosis. *Int J Adv Robot Syst* 10:359
54. Veneman JF, Ekkelenkamp R, Kruidhof R et al (2006) A series elastic- and Bowden-cable-based actuation system for use as torque actuator in exoskeleton-type robots. *Int J Robot Res* 25:261–281. doi:[10.1177/0278364906063829](https://doi.org/10.1177/0278364906063829)
55. Wyeth G (2008) Demonstrating the safety and performance of a velocity sourced series elastic actuator. In: Proceedings of the IEEE international conference on robotics and automation, 19–23 May, Pasadena, CA, USA, pp 3642–3647, doi: [10.1109/ROBOT.2008.4543769](https://doi.org/10.1109/ROBOT.2008.4543769)
56. Yoon S, Kang S, Kim S et al (2003) Safe arm with MR-based passive compliant joints and visco-elastic covering for service robot applications. In: Proceedings of the 2003 IEEE/RSJ international conference on intelligent robots and systems (IROS 2003), 27–31 October, Las Vegas, USA, vol 3, pp 2191–2196, doi: [10.1109/IROS.2003.1249196](https://doi.org/10.1109/IROS.2003.1249196)
57. Carpino G, Accoto D, Sergi F et al (2012) A novel compact torsional spring for series elastic actuators for assistive wearable robots. *J Mech Design* 134:121002. doi:[10.1115/1.4007695](https://doi.org/10.1115/1.4007695)
58. Robinson D (2000) Design and analysis of series elasticity in closed-loop actuator force control. PhD dissertation, Massachusetts Institute of Technology (MIT), Cambridge
59. Van Ham R, Sugar T, Vanderborght B et al (2009) Compliant actuator designs. *IEEE Robot Automat Mag* 16:81–94. doi:[10.1109/MRA.2009.933629](https://doi.org/10.1109/MRA.2009.933629)
60. Tagliamonte NL, Sergi F, Accoto D et al (2012) Double actuation architectures for rendering variable impedance in compliant robots: a review. *Mechatronics* 22:1187–1203. doi:[10.1016/j.mechatronics.2012.09.011](https://doi.org/10.1016/j.mechatronics.2012.09.011)
61. Accoto D, Carpino G, Tagliamonte NLT, Sergi F et al (2012) pVEJ: a modular passive viscoelastic joint for assistive wearable robots. In: 2012 IEEE international conference on robotics and automation (ICRA), 14–18 May, St. Paul, Minnesota, USA, pp 3361–3366
62. Carpino G, Accoto D, Di Palo M et al (2011) Design of a rotary passive viscoelastic joint for wearable robots. In: 2011 IEEE international conference on rehabilitation robotics (ICORR), June 29–July 1, Zurich, Switzerland, pp 1–6
63. Siciliano B, Sciavicco L (2009) Robotics: modelling, planning and control. Springer-Verlag London
64. Whitney DE (1987) Historical perspective and state of the art in robot force control. *Int J Rob Res* 6:3–14. doi:[10.1177/027836498700600101](https://doi.org/10.1177/027836498700600101)
65. Salisbury JK (1980) Active stiffness control of a manipulator in Cartesian coordinates. In: 1980 19th IEEE conference on decision and control including the symposium on adaptive processes, 10–12 December, Albuquerque, NM, vol 19, pp 95–100, doi: [10.1109/CDC.1980.272026](https://doi.org/10.1109/CDC.1980.272026)
66. Hogan N (1985) Impedance control: an approach to manipulation: Parts I, II, and III. *J Dyn Syst Measure Control* 107:1–24

67. Raibert MH, Craig JJ (1981) Hybrid position/force control of manipulators. *Trans ASME J Dyn Syst Meas Contr* 102:126–133
68. Adams RJ, Hannaford B (2002) Control law design for haptic interfaces to virtual reality. *IEEE Trans Control Syst Technol* 10:3–13. doi:[10.1109/87.974333](https://doi.org/10.1109/87.974333)
69. Colgate E, Hogan N (1989) An analysis of contact instability in terms of passive physical equivalents. In: *Proceedings of the 1989 IEEE international conference on robotics and automation*, 14–19 May, Scottsdale, AZ, USA, vol 1, pp 404–409
70. Eppinger S, Seering W (1987) Understanding bandwidth limitations in robot force control. In: *Proceedings of the 1987 IEEE international conference on robotics and automation*, 31 March–3 April, Raleigh, NC, USA, pp 904–909
71. Albu-Schaffer A, Ott C, Hirzinger G (2007) A Unified Passivity-based Control Framework for Position, Torque and Impedance Control of Flexible Joint Robots. *The International Journal of Robotics Research* 26:23–39. doi:[10.1177/0278364907073776](https://doi.org/10.1177/0278364907073776)
72. Hogan N (1989) Controlling impedance at the man/machine interface. In: *Proceedings of the 1989 IEEE international conference on robotics and automation*, 14–19 May, Scottsdale, AZ, USA, vol 3, pp 1626–1631
73. Pratt G, Williamson M (1995) Series elastic actuators. *Intelligent robots and systems* 95. In: *Proceedings of the 1995 IEEE/RSJ international conference on human robot interaction and cooperative robots*, 5–9 August, Pittsburgh, Pennsylvania, USA, vol 1, 399–406, doi:[10.1109/IROS.1995.525827](https://doi.org/10.1109/IROS.1995.525827)
74. Pratt G, Willisson P, Bolton C, Hofman A (2004) Late motor processing in low-impedance robots: impedance control of series-elastic actuators. In: *Proceedings of the 2004 American control conference*, 30 June–2 July, Boston, MA, vol 4, pp 3245–3251, doi:[10.1109/ACC.2004.182786](https://doi.org/10.1109/ACC.2004.182786)
75. Kong K, Bae J, Tomizuka M (2009) Control of rotary series elastic actuator for ideal force-mode actuation in human–robot interaction applications. *IEEE/ASME Trans Mechatronics* 14:105–118. doi:[10.1109/TMECH.2008.2004561](https://doi.org/10.1109/TMECH.2008.2004561)
76. Grun M, Muller R, Konigorski U (2012) Model based control of series elastic actuators. In: *2012 4th IEEE RAS EMBS international conference on biomedical robotics and biomechatronics (BioRob)*, 24–27 June, Rome, Italy, pp 538–543
77. Vallery H, Ekkelenkamp R, Van der Kooij H, Buss M (2007) Passive and accurate torque control of series elastic actuators. In: *Proceedings of IEEE IROS, IEEE/RSJ International Conference on Intelligent Robots and Systems*, October 29–November 2, San Diego, USA, pp 3534–3538
78. Krebs HI, Hogan N, Aisen ML, Volpe BT (1998) Robot-aided neurorehabilitation. *IEEE Trans Rehabil Eng* 6:75–87. doi:[10.1109/86.662623](https://doi.org/10.1109/86.662623)
79. Schaechter J (2004) Motor rehabilitation and brain plasticity after hemiparetic stroke. *Progress Neurobiol* 73:61–72
80. Gordon KE, Ferris DP (2007) Learning to walk with a robotic ankle exoskeleton. *J Biomech* 40:2636–2644. doi:[10.1016/j.jbiomech.2006.12.006](https://doi.org/10.1016/j.jbiomech.2006.12.006)
81. Rossini PM, Micera S, Benvenuto A et al (2010) Double nerve intraneural interface implant on a human amputee for robotic hand control. *Clin Neurophysiol* 121:777–783. doi:[10.1016/j.clinph.2010.01.001](https://doi.org/10.1016/j.clinph.2010.01.001)
82. Kiguchi K, Iwami K, Yasuda M et al (2003) An exoskeletal robot for human shoulder joint. *IEEE/ASME Trans Mechatronics* 8:125–135
83. Lenzi T, De Rossi SMM, Vitiello N, Carrozza MC (2012) Intention-based EMG control for powered exoskeletons. *IEEE Trans Biomed Eng* 59:2180–2190. doi:[10.1109/TBME.2012.2198821](https://doi.org/10.1109/TBME.2012.2198821)
84. Rosen J, Brand M, Fuchs MB, Arcan M (2001) A myosignal-based powered exoskeleton system. *IEEE Trans Syst Man Cybernetics Part A Syst Hum* 31:210–222. doi:[10.1109/3468.925661](https://doi.org/10.1109/3468.925661)
85. Cavallaro EE, Rosen J, Perry JC, Burns S (2006) Real-time myoprocessors for a neural controlled powered exoskeleton arm. *IEEE Trans Biomed Eng* 53:2387–2396. doi:[10.1109/TBME.2006.880883](https://doi.org/10.1109/TBME.2006.880883)



86. Kinnaird CR, Ferris DP (2009) Medial gastrocnemius myoelectric control of a robotic ankle exoskeleton. *IEEE Trans Neural Syst Rehabil Eng* 17:31–37. doi:[10.1109/TNSRE.2008.2008285](https://doi.org/10.1109/TNSRE.2008.2008285)
87. Dietz V, Fouad K, Bastiaanse CM (2001) Neuronal coordination of arm and leg movements during human locomotion. *Eur J Neurosci* 14:1906–1914. doi:[10.1046/j.0953-816x.2001.01813.x](https://doi.org/10.1046/j.0953-816x.2001.01813.x)
88. Rueterbories J, Spaich EG, Larsen B, Andersen OK (2010) Methods for gait event detection and analysis in ambulatory systems. *Med Eng Phys* 32:545–552. doi:[10.1016/j.medengphy.2010.03.007](https://doi.org/10.1016/j.medengphy.2010.03.007)
89. Novak D, Reberšek P, De Rossi SMM, Donati M, Podobnik J, Beravs T, Lenzi T, Vitiello N, Carrozza MC, Munih M (2013) Automated detection of gait initiation and termination using wearable sensors. *Med Eng Phys* 35(12):1713–1720. doi:[10.1016/j.medengphy.2013.07.003](https://doi.org/10.1016/j.medengphy.2013.07.003)
90. Ronsse R, Vitiello N, Lenzi T et al (2011) Human-robot synchrony: flexible assistance using adaptive oscillators. *IEEE Trans Biomed Eng* 58:1001–1012. doi:[10.1109/TBME.2010.2089629](https://doi.org/10.1109/TBME.2010.2089629)
91. Righetti L, Buchli J, Ijspeert AJ (2006) Dynamic Hebbian learning in adaptive frequency oscillators. *Physica D Nonlinear Phenom* 216:269–281. doi:[10.1016/j.physd.2006.02.009](https://doi.org/10.1016/j.physd.2006.02.009)
92. Righetti L, Buchli J, Ijspeert AJ (2009) Adaptive frequency oscillators and applications. *Open Cybernetics Syst J* 3:64–69. doi:[10.2174/1874110X00903020064](https://doi.org/10.2174/1874110X00903020064)
93. Ronsse R, Lenzi T, Vitiello N et al (2011) Oscillator-based assistance of cyclical movements: model-based and model-free approaches. *Med Biol Eng Comput* 49:1173–1185. doi:[10.1007/s11517-011-0816-1](https://doi.org/10.1007/s11517-011-0816-1)
94. Tagliamonte NL, Sergi F, Carpino G et al (2013) Human-robot interaction tests on a novel robot for gait assistance. In: *IEEE International Conference on Rehabilitation Robotics (ICORR)*, 24–26 June 2013, Seattle, WA, pp. 1–6.
95. Vallery H, Veneman J, Van Asseldonk E et al (2008) Compliant actuation of rehabilitation robots: benefits and limitations of Series Elastic Actuators. *IEEE Robot Automat Mag* 15:60–69. doi:[10.1109/MRA.2008.927689](https://doi.org/10.1109/MRA.2008.927689)
96. Pintelon R, Schoukens J (2001) *System identification: a frequency domain approach*. IEEE Press, New York